



ChemTech

## International Journal of ChemTech Research

CODEN (USA): IJCRGG, ISSN: 0974-4290, ISSN(Online):2455-9555  
Vol.10 No.7, pp 350-358, 2017

### Hydrothermal Synthesis of Mesoporous sulphated Zirconia

Amit Kumar<sup>1\*</sup>, ShaileySinghal<sup>2</sup>, ShilpiAgarwal<sup>3</sup>, RajendraPrasadBadoni<sup>4</sup>,  
Amitabh Raj Tripathi<sup>5</sup>

<sup>1,2,3</sup>Department of Chemistry, College of Engineering Studies, University of Petroleum & Energy Studies, Dehradun (Uttarakhand), India.

<sup>4</sup>Department of Chemical Engineering, College of Engineering Studies, University of Petroleum & Energy Studies, Dehradun (Uttarakhand), India.

<sup>5</sup>Environmental management division, Central pulp and paper research institute, Saharanpur (Uttara Pradesh), India.

**Abstract :** The present study focus on synthesis to obtain mesoporous zirconia and sulphated zirconia has been developed. Sulphated zirconia has been prepared by two step synthesis by hydrothermal route and calcined at 600°C, wherein sulphate moiety has been introduced on support. Sulphated zirconia has many important industrial applications especially in field of oil industry as catalyst. Obtained zirconia and sulphated zirconia has been characterized for BET surface area, pore volume & pore size distribution by nitrogen adsorption/ desorption method, NH<sub>3</sub>-TPD, H<sub>2</sub>-TPR, X-ray diffraction (XRD), Fourier transmission spectroscopy (FTIR) Thermogravimetric analysis (TGA) and Scanning electron microscope (SEM). The prepared zirconia materials are crystalline in nature and high surface area (225 m<sup>2</sup>/g and higher acidic (7.15ml/g).

**Keywords :** Zirconia; sulphated zirconia; hydrothermal; BET; TPD/TPR.

#### 1 Introduction

Metal oxides are a class of outstanding category of solid catalyst widely used as support for several reactions. [1]. among these oxides zirconium oxide (ZrO<sub>2</sub>) is very promising as catalyst support [2–4]. Zirconia exists in three crystalline forms, obtained at different temperature ranges, viz. monoclinic 400°C-1170°C, tetragonal 1170°C - 2370°C and cubic 2370°C -2680°C. Above 2680°C zirconia is in liquid form. It should be noted that a metastable tetragonal phase also exists at room temperature that is transformed into thermodynamically stable monoclinic phase upon heat treatment.

The formation of crystal structure in materials depends upon its atoms mobility behaviour. High temperature and pressure are two parameters that had been used constantly to control and adjust this mobility behaviour. Crystallinity of sample is also an important property, as amorphous samples generally do not perform well due to lack of active sites at the surface [5, 6]. Recently, ZrO<sub>2</sub> has received considerable attention as a catalyst for various reactions, hydrodechlorination of dichloromethane [7], benzylation of anisole [8], Isomerization of n-hexane [9], cracking [10], dehydrogenation [11-12] and hydrodesulphurization [13]. This specific behaviour of ZrO<sub>2</sub> in these reactions is due to a special combination of surface properties, namely the preservation of both acidic and basic sites for reduction–oxidation properties and also high thermal stability [14-16].

ZrO<sub>2</sub> has low specific surface area and more expensive than traditional oxides, such as: alumina (Al<sub>2</sub>O<sub>3</sub>)

and silica (SiO<sub>2</sub>). For these reasons, some researchers have focused its studies on the stabilization of highly dispersed ZrO<sub>2</sub> on a high surface area support. ZrO<sub>2</sub> dispersed on a support as alumina could constitute a new class of catalyst support combining the chemical properties of zirconia with the high surface area and the mechanical stability of the supports [17,]. Some authors have reported the preparation and characterization of zirconia on alumina [18]. Methods of synthesis for obtaining ZrO<sub>2</sub> with at high surface area and desirable physical, chemical and structural characteristics are still the subject of concern.

In this paper, we report the synthesis of ZrO<sub>2</sub> by hydrothermal route. The influence of synthesis conditions were evaluated on the structure and morphology of mesoporous zirconia. Nano powders obtained were analysed by X-ray diffraction (XRD), adsorption-desorption N<sub>2</sub> -isotherms, Fourier transform infrared (FT-IR) spectroscopy, Temperature program desorption (NH<sub>3</sub>-TPD), Temperature program reduction (H<sub>2</sub>-TPR), scanning electron microscopy (SEM) and Thermogravimetric analysis (TGA).

## 2 Experimental Sections

### 2.1 Materials and methods

All the chemicals used in this work were of analytical reagent grade. Zirconium oxychloride was from Loba Chemie India, ammonium hydroxide was from Renkem India, and sulphuric acid was from Fischer Scientific India. Double distilled water was used for preparation of all solutions.

### 2.2 Preparation of ZrO<sub>2</sub>

Prepared 0.5M concentration zirconium oxychloride solution in distilled water and take 250 ml of zirconium oxychloride solution in two neck round bottom flask and continuous stirring at 600 rpm. It was then precipitated by the dropwise addition of ammonium hydroxide (30%) until pH 10. The precipitate was transferred to the teflon autoclave and heated at 150°C for 5hr. The autoclave was cooled down to room temperature and then the precipitate was filtered and washed till that the pH did not reduce from 10 to 7 and the filtrate was not free from chloride ions. The presence of chloride ions was detected by (silver nitrate) solution. The precipitate cake was dried in hot air oven at 120°C overnight, slightly crushed and sieved to 100µm. The dried sample was calcined in muffle furnace at 600°C for 4 hr at the rate 1°C/min.

### 2.3 Preparation of S-ZrO<sub>2</sub>

The ZrO<sub>2</sub> was dispersed in 0.5M aqueous sulphuric acid. 15 ml of sulfuric acid solution was added to 1g of zirconia by dropwise addition [19, 20,] with 600rpm for 1 hr at room temperature, filtered and dried at 120°C for overnight, then calcined at 600°C for 4hr and referred as S-ZrO<sub>2</sub>.

## 3. Characterization

X-ray diffraction patterns were measured on Bruker Advance D8 X ray diffractometer and CuK<sub>α</sub> contribution was eliminated by CuK<sub>α</sub> radiation with  $\lambda = 1.541 \text{ \AA}$ ). The Applied voltage used in the instrument was 40Kv, current 30mA. The  $\theta$  range was  $2\theta = 15$  to  $80^\circ$ . The X-ray data was collected with a scan rate of  $10^\circ \text{ min}^{-1}$  and a step size of  $0.2^\circ$ . The morphology of the mixed oxides was identified by scanning electron microscopy (SEM, SERON Technology, Korea) using 20 KVA. Fourier transform infrared spectroscopy (FTIR) was performed with Perkin Elmer instrument to examine the linkages between zirconia and heterometal oxide network, the samples first was prepared as pastilles with KBr, in the proportion of 1% of the solids. The surface area measured by Brunauer-Emmett-Teller (BET) method at liquid nitrogen temperature, pore size distributions determine with the desorption branch of isotherm, and average particle size was also measured by nitrogen adsorption/desorption isotherm at 77K using Accelerated Surface Area and Porosimetry System, Micromeritics, (ASAP 2020) [32]. Before the measurement all the samples were degassed at 250°C for 6 hr. The temperature-programmed desorption profile of ammonia (NH<sub>3</sub>-TPD) over the material was carried out in a U type quartz reactor (ID = 6 mm). 0.1 g of material placed above the quartz wool with a Micromeritics Chemisorb 2750 instruments. The samples first were pre-treated under argon flow ( $20 \text{ ml min}^{-1}$ ) for two hours at 150°C, cool down the temperature at room temperature. After pre-treatment, the samples were submitted to a chemisorption step using mixture of ammonia in helium (9.8%, mol/mol) flow of  $20 \text{ ml min}^{-1}$  at room temperature, for 30 minutes. Thereafter, the system was flushed with helium at room temperature for two hours in order to remove extra

ammonia molecules in the material surface; the material was treated for 30 minutes at 120°C under helium flow (20ml min<sup>-1</sup>). This step was followed by temperature programmed desorption analysis; the sample was heated from 100 to 900°C, at a rate of 10°C min<sup>-1</sup> and helium as carrier gas (20 ml min<sup>-1</sup>). The desorbed ammonia amount was detected with thermal conductivity detector (TCD) [32]. The temperature program reduction profile carried out in same instrument using the mixture of hydrogen and argon (9.8% H<sub>2</sub> in Argon) as above for TPD. The thermogravimetric analysis was carried out in SDT Q600 V8.3101 TG-DTA instrument, the small amount of sample was placed onto platinum crucible and the analysis was carried out under N<sub>2</sub> flow at the heating rate of 10°C min<sup>-1</sup>, in the temperature range from room temperature to 900°C.

## 4. Result and discussion

### 4.1 Morphology and X-Ray Diffraction

SEM images show that the particles obtained by hydrothermal method are distributed uniformly with equal grain size. It is clear from the image that the particles of zirconia are spherical with same size, homogeneously distributed, although. The similar morphology is observed in case of SZ, Presence of sulphate ions reflected in the form of more agglomerated. The images were taken at magnification at X10K with grain size 1µm.

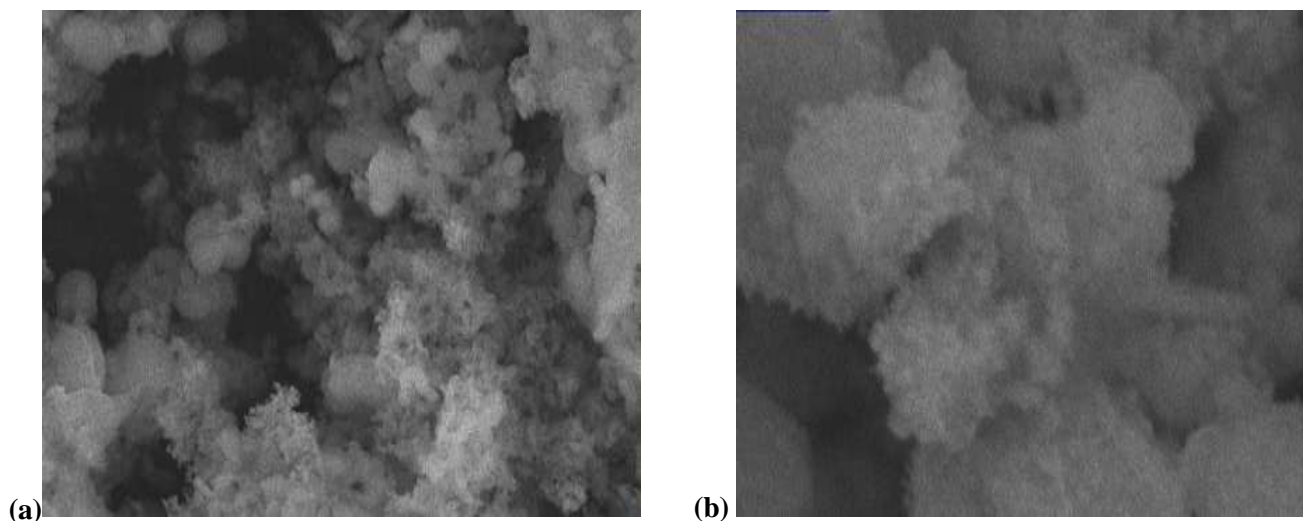


**Figure 1 SEM Image (a) Z (b) SZ**

XRD pattern of uncalcined ZrO<sub>2</sub> zirconia are amorphous, while calcined zirconia (ZrO<sub>2</sub>) and sulfated zirconia (S-ZrO<sub>2</sub>) are in crystalline phase. The most Intense peaks were obtained at 2θ = 30.13°, 35.36°, 50.40°, 60.2°, 62.83° and 74.5° represent to the tetragonal phase of zirconia, corresponding to (101), (110), (112), (200), (211), (202) and (220) planes (JCPDS card number 80-2155), respectively [21]. Some additional peaks in the pattern of zirconia shows at 2θ = 24.50°, 28.36°, 31.4°, 34.3°, 41.55°, 45.59°, 54.10°, 55.54° and 65.75°, which are evidence of the monoclinic phase (JCPDS card number 7-3430). These results suggest that tetragonal and monoclinic phases coexisted in the materials. The crystallite sizes D of the samples were calculated using the Scherrer equation (1).

$$D = \frac{0.9\lambda}{\beta \cos \theta} \quad (1)$$

Where λ is the wavelength radiation used (λ = 1.5406 Å), θ is the Bragg angle and β is the line width at half maximum height calculated from the full width at half maximum intensity (FWHM). The average crystallite size of these materials was around 27 nm.

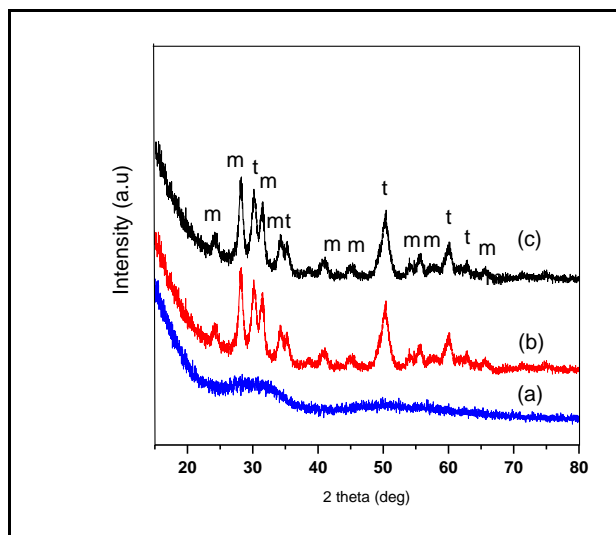


Figure 2 XRD of the materials (a) uncalcined  $ZrO_2$  (b)  $ZrO_2$  (S- $ZrO_2$ )

#### 4.2 FTIR

The FT-IR spectra of pure  $ZrO_2$  and sulfated zirconia calcined at  $600^\circ C$  were measured in the range  $4000-400\text{ cm}^{-1}$  (Fig. 2). In the FT-IR spectrum for pure  $ZrO_2$ , the bands at  $423-654\text{ cm}^{-1}$  correspond to Zr-O-Zr bond [16]. A strong and broad band with at  $3398\text{ cm}^{-1}$  is attributed to physisorbed water, whereas the band at  $1635\text{ cm}^{-1}$  can be assigned to the bending mode (H-O-H) of coordinated water [22]. Band at  $1362\text{ cm}^{-1}$  was assigned to the bending vibration of Zr-OH groups [23]. The FT-IR spectra of sulfated zirconia show bands at  $1053, 1120$  and  $1224\text{ cm}^{-1}$ . These bands are assigned to asymmetric and symmetric stretching modes of oxygen bound to the sulfur of sulfate [24]. Moreover, the band at  $1429\text{ cm}^{-1}$  is due to the presence of S-O stretching vibration of the surface sulfate species [25]. The wave number of this band increases with the sulfur content, due to change in the type of sulfate species from isolated ones to polynuclear ones [26]. The partially ionic nature of the S-O bond is responsible for the Bronsted acid sites in sulfated zirconia samples [27]. Furthermore, the band observed at  $1636\text{ cm}^{-1}$  is due to the bending vibration mode of an O-H group of water associated with the sulfate. The broad band around  $3200\text{ cm}^{-1}$  is attributed to the O-H stretching vibration of water associated with  $ZrO_2$  and the broadness indicates the effect of hydrogen bonding [28]. It is worth mentioning here that the O-H stretching, vibration band decreases by the increasing percentage loading of  $SO_4^{2-}$ . This behavior may be attributed to the successive formation of  $H_2SO_4, HSO_4^-$  and  $SO_4^{2-}$  from water sensitive  $SO_3$  groups [29].

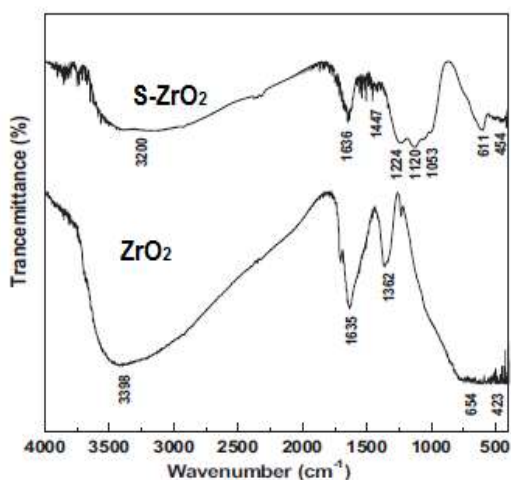


Figure 3 FTIR spectra of sample (a)  $ZrO_2$  (b) S- $ZrO_2$

### 4.3 Nitrogen adsorption/Desorption

$N_2$  adsorption-desorption isotherms for zirconia and sulphated zirconia are given in Figure 3a. The isotherm show well defined hysteresis loops ( $H_3$  Type) for the zirconia samples. The material show mesopore due to the occurrence of conspicuous hysteresis loops at high relative pressures and non-rigid aggregates of plate-like particles (slit-shaped pores) being related to weak interaction and capillary condensation associated with large pore channels [30, 32]. Among the synthesized oxides, it has been observed that the relative pressure point, where adsorption and desorption branches coincide, is affected by the type of the metal oxide present and it was found to have hysteresis at highest relative pressure. Pure zirconia showed hysteresis at highest relative pressure, showing the presence of maximum pore volume and sulphated zirconia show hysteresis at lower relative pressure which is the evidence of less pore volume. The PSD of the final product indicates the Pure zirconia have wider pore size distribution and sulphated zirconia show shorter pore size distribution. The intercalation of oxides and reduction of particle size to nano range could help in achieving high surface area with appreciable pore volume. Figure 3b shows the pore size distribution of samples.

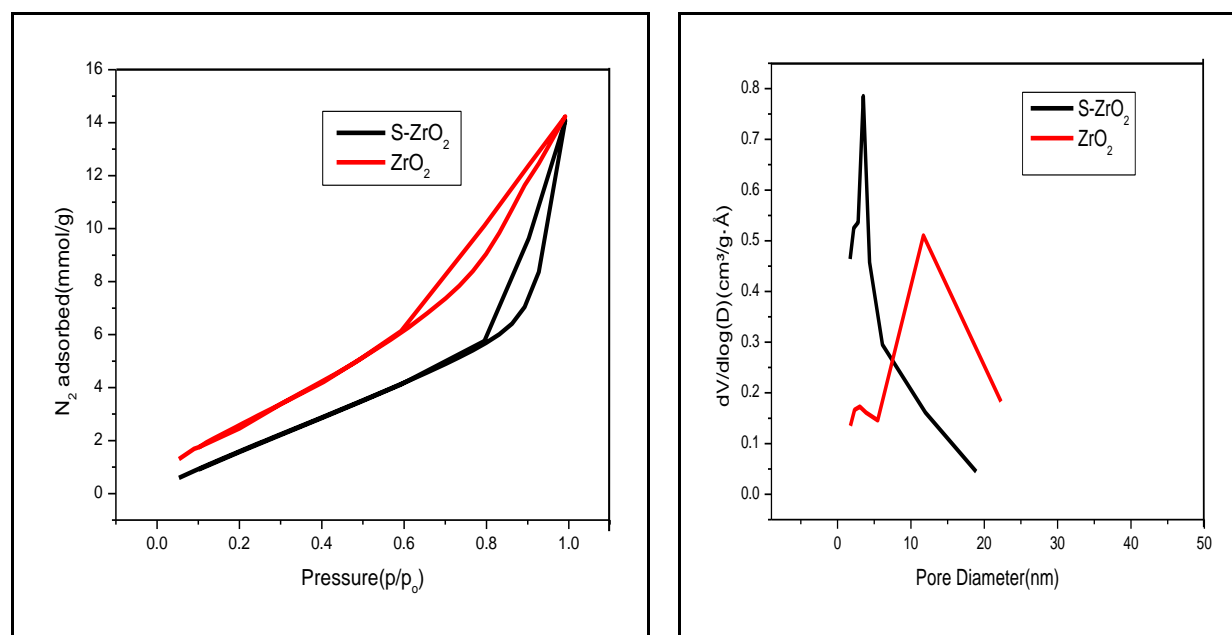


Figure 4.(a)  $N_2$  adsorption/desorption isotherm (b) Pore size distribution

### 4.4 $NH_3$ – TPD

The concentration and strength of the acid sites of the material was evaluated by  $NH_3$ -TPD (i.e. expressed as an amount of  $NH_3$  desorbed per gram of catalyst) and presented in Table 1. The  $NH_3$ -TPD profiles of the ZrO<sub>2</sub> and S-ZrO<sub>2</sub> material are shown in Fig.5. The profile of ammonia TPD indicates the presence of acid sites of different strengths in the materials. The desorption peaks of the TPD in the materials located at 100–200 °C, 200–400 °C and >400 °C can be assigned to weak, moderate, strong and very strong acid sites, respectively[31, 32].

It is cleared from the profile of TPD, all the weak, moderate and strong acid sites are present in the both the materials. However, the strong acid sites with characteristic desorption temperature of about 450 °C were observed in ZrO<sub>2</sub> and S-ZrO<sub>2</sub>.

Table 1 Characteristics of oxides:

Sample	$S_A$ (m <sup>2</sup> /g)	$V_P$ (cc/g)	$D_P$ (nm)	$S_P$ (nm)	$A_T$ ml/g)	Crystallinity
ZrO <sub>2</sub>	225	0.49	7.89	27.25	3.03	Crystalline
S-ZrO <sub>2</sub>	235	0.44	6.73	25.40	7.15	Crystalline

$S_A$ : Surface area,  $V_P$ : Pore volume,  $D_P$ : Average pore diameter,  $S_P$ : Average particle size,  $A_T$ : Total acidity

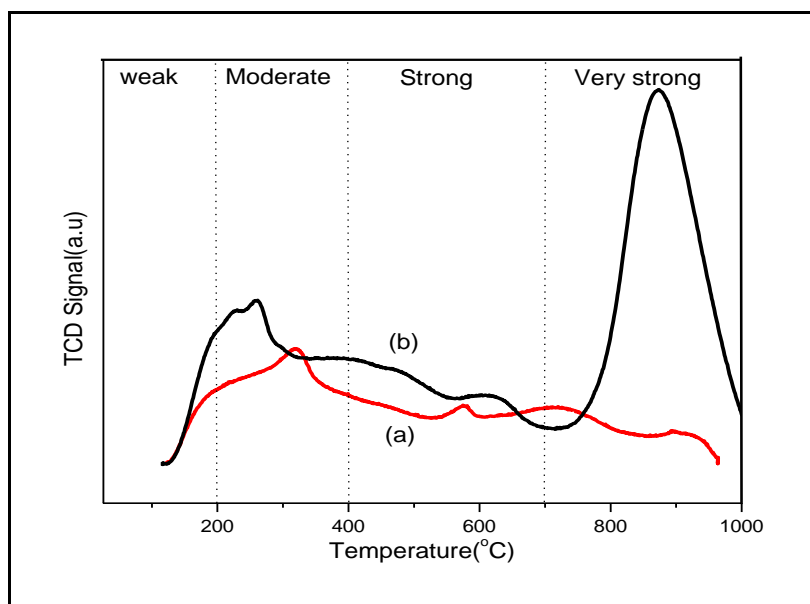


Figure 5 NH<sub>3</sub>-TPD of sample (a) ZrO<sub>2</sub> (b) S-ZrO<sub>2</sub>

#### 4.5 H<sub>2</sub> – TPR

The redox properties of ZrO<sub>2</sub> and S-ZrO<sub>2</sub> materials were evaluated by temperature-programmed reduction (TPR) with 10% H<sub>2</sub>/Ar (30 mL min<sup>-1</sup>). Fig. 6 show the TPR profiles of ZrO<sub>2</sub> and S-ZrO<sub>2</sub> material, where the peak maximum indicates the temperature corresponding to the maximum rate of reduction. The reduction peak of zirconia and sulphated zirconia was obtained at 557°C and 576°C respectively.

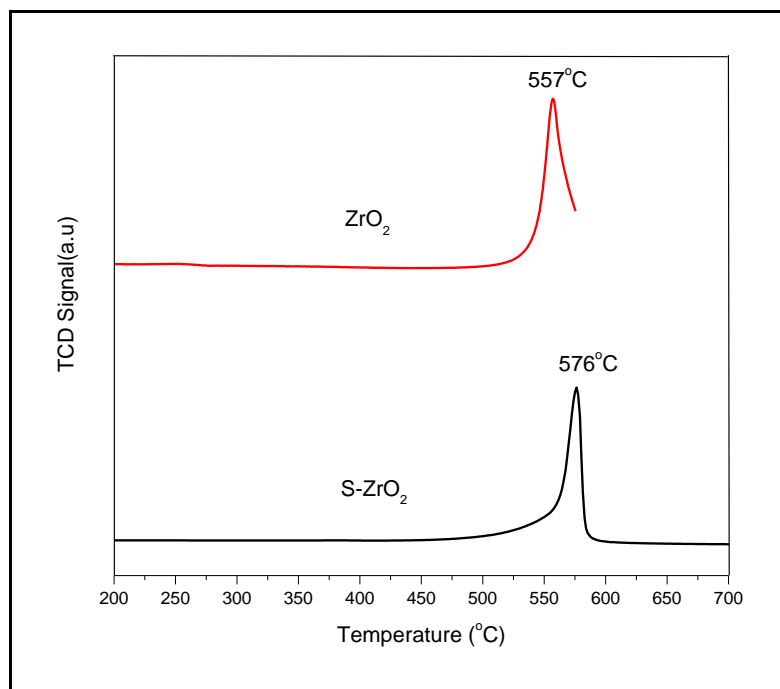
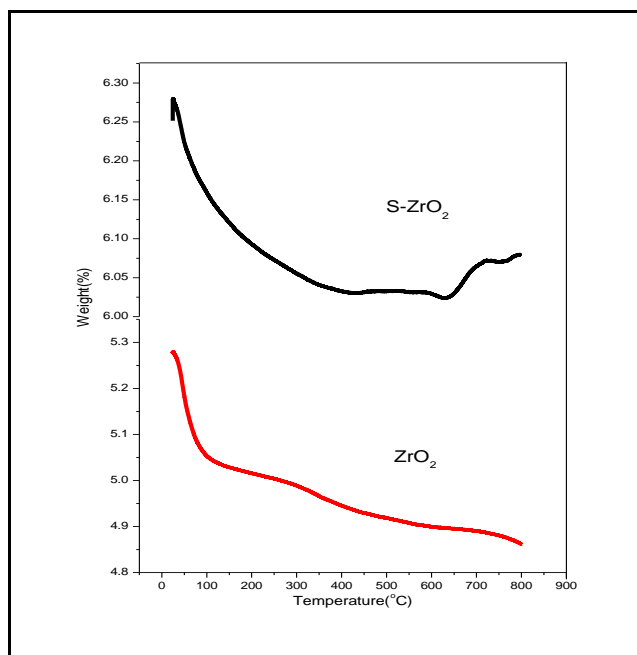


Figure 6 H<sub>2</sub>-TPR of sample (a) ZrO<sub>2</sub> (b) S-ZrO<sub>2</sub>

#### 4.6 Thermogravimetric analysis (TGA)

Thermal properties of zirconia and sulphated zirconia (Fig.7) showed three stages of weight loss, between 25°C to 800°C. First weight loss between 25°C and 110°C was indicative of the removal of surface physisorbed water molecules, and the second mass loss (approximately between 290°C and 450°C) was due to

dehydroxylation of zirconyl hydroxide. Third stage between 450°C and 800°C of weight reduction was assigned to the dehydration of hydrated zirconium oxide. The trend of loss of water suggested the conversion of zirconium hydroxide to zirconia [33, 34]. In case of sulphated zirconia various mass loss steps were obtained (Fig 7); the first step (25°C to 110°C) was attributed to the removal of physically adsorbed water, whereas the other three stages, between 250 to 520°C due to the dehydration process. The mass loss at higher temperature, between 670°C to 730°C was correspond to the decomposition of sulphate group [35, 36]. The complete TGA profile responding to loss of 5% Sulphate ions by weight from sulphated zirconia. TGA studies also suggest the stability of the prepared catalyst till 600°C.



**Figure 7 TGA Curve of zirconia**

## 5. Conclusion.

Zirconium oxide ( $ZrO_2$ ) has been prepared by hydrothermal method. Results indicate the viability of the method to obtain mesoporous oxide with high surface area and acidity. The material comprised of high surface area, good pore volume and acceptable acidity and bulk density, however sulphate ion responded to increase in surface area, and acidity. It is important to mention that high surface area is the foremost required characteristic of an effective catalyst. By adopting hydrothermal method, samples with very high surface area ( $225\text{cm}^2/\text{g}$ ) higher pore volume ( $0.49\text{cc/g}$ ) can be produced, which can be used as good support material for various catalytic reactions. High surface area with good pore volume and pore size will enhance the probability of the material for specific reactions (Isomerization of light alkanes).

## Acknowledgements

Authors feel great pleasure to express their inexplicable & deep sense of gratitude to the Chancellor Dr. S. J. Chopra, Vice Chancellor Dr. Shrihari Honwad, Dean Dr. Kamal Bansal and Head, Department of Chemistry Dr. Pankaj Kumar Thakur for their continuous support and encouragement.

## Conflict of Interest

No conflict of interest

## 6. References

1. C. Burda, X. Chen, R. Narayanan, M.A. El-Sayed, Chemistry and Properties of Nanocrystals of Different Shapes *Chem. Rev.* 105(4) (2005) 1025-1102

2. F. Noronha, E. Fendley, R. Soares, W. Alvarez, D. Resasco, Correlation between catalytic activity and support reducibility in the CO<sub>2</sub> reforming of methane over Pt/Ce<sub>x</sub>Zr<sub>1-x</sub>O<sub>2</sub> catalysts *Chem. Eng. J.* 82 (2001) 21-31
3. S. Irusta, L. M. Cornaglia, and E. A. Lombardo, Hydrogen Production Using Ni–Rh on ZrO<sub>2</sub> as Potential Low-Temperature Catalysts for Membrane Reactors, *Journal of Catalysis* 210, (2002)263–272
4. M.A. Arribas, F. Márquez, A. Martinez, Activity, Selectivity, and Sulfur Resistance of Pt/WO<sub>x</sub>–ZrO<sub>2</sub> and Pt/Beta Catalysts for the Simultaneous Hydro isomerization of *n*-Heptane and Hydrogenation of Benzene, *J. Catal.* 190(2) (2000) 309-319
5. G. Dercz, Prusik, and L. Pajak, “X-Ray and SEM Studies on Zirconia Powder,” *Journal of Achievement in Materials and Manufacturing Engineering*, [31, (2008), 408-414.
6. D.H. Aguilar, L.C. Torres-Gonzalez, L.M. Torres-Martinez, T. Lopez, P. Quitina, A Study of the Crystallization of ZrO<sub>2</sub> in the Sol–Gel System: ZrO<sub>2</sub>–SiO<sub>2</sub>, *J. Solid State Chem.* 158 (2001) 349-357.
7. J. Bedia, L.M. Gomez-Sainero, J.M. Grau, M. Busto, M. Martin-Martinez, J.J. Rodriguez, Hydrodechlorination of dichloromethane with mono- and bimetallic Pd–Pt on sulfated and tungstated zirconia catalysts, *journal of catalysis*, 294, 2012, 207-215
8. Pratap T Patil, Kusum M Malshe, Pradeep Kumar, Mohan K Dongare, Erhard Kemnitz, Benzoylation of anisole over borate zirconia solid acid catalyst, *Catalysis Communications*, 3( 9),( 2002), 411-416.
9. R. Silva-Rodrigo, E.L. Cruz-Dominguez, F.E. Lugo-del Angel, J. Navarrete-Bolanos, R. Garcia-Alamilla, A. Olivas-Sarabia, J.A. Melo-Banda, L.C. Cruz-Netro, G. Zamora-Ramirez, A. Castillo-Mares, Studies of sulphated mixed oxides (ZrO<sub>2</sub>–SO<sub>4</sub>–La<sub>2</sub>O<sub>3</sub>) in the isomerization of *n*-hexane, *Catalysis Today*, 250, ( 2015) 197-208.
10. M. Busto, M.E. Lovato, C. R. Vera, K. Shimizu, J. M. Grau, Silica supported tungsta-zirconia catalysts for hydro isomerization–cracking of long alkanes, *Applied catal A Gen*, 355(1-2)(2009)123-131
11. M.G. Cutrufello, S.D Rossi, I. Ferino, R. Monaci, E. Rombi, V. Solinas, Preparation, characterisation and activity of chromia–zirconia catalysts for propane dehydrogenation, *Thirmochimica acta*, 434(2005), 62-68
12. A. Verma, R. Dwivedi, P. Sharma, R. Prasad, Oxidative dehydrogenation of ethylbenzene to styrene over zirconium vanadate catalyst prepared by solution combustion method, *RSC Adv.*, 4(2014), 1799-1807.
13. L. Kaluza, M. Zdrzil, Preparation of zirconia supported hydrodesulphurization catalyst by water assisted spreading *Applied Catalyst A: gen* 339 (2007), 58-67.
14. K. Tanabe, Surface and catalytic properties of ZrO<sub>2</sub>, *Mater. Chem. Phys.* 13 (1985) 347-364.
15. K. Tanabe, M. Misono, Y. Ono, H. Hattori, Definition and Classification of Solid Acids and Bases, *Stud. Surf. Sci. Catal.* 51 (1989) 1-3.
16. T. Yamaguchi, Recent progress in solid super acid, *Appl. Catal.* 61 (1990) 1-25.
17. S. Damyanova, P. Grange, B. Delmon, Surface Characterization of Zirconia-Coated Alumina and Silica Carriers, *journal of catalysis*, 168(2) 1997, 421-430.
18. J. Chandradass, J.H. Yoon, D.S. Bae, Synthesis and characterization of zirconia doped alumina nanopowder by citrate–nitrate process *Mater. Sci. Eng. A.* 473 (2008) 360.
19. C. Zhang, R. Miranda, B.H. Davis, Platinum-sulfated-zirconia. Infrared study of adsorbed pyridine, *Catalysis let* 1994: 29; 349-359.
20. K. Saravanam, B. tyagi, H.C. Bajaj, Catalytic activity of sulphated zirconia solid acid catalyst for esterification of myristic acid with methanol, *Ind j of chem.*, 53 (2014) 199-805
21. F. Heshmatpour, R.B. Aghakhanpour, Synthesis and characterization of superfine pure tetragonal nanocrystalline sulfated zirconia powder by a non-alkoxide sol–gel route, *Adv. Powder Technol.* 23 (2012) 80–87.
22. S. Gowri, R. Rajiv Gandhi, M. Sundrarajan, Structural, Optical, Antibacterial and Antifungal Properties of Zirconia Nanoparticles by Biobased Protocol, *J. Mater. Sci. Technol.*, 30(8), (2014), 782-790
23. Sinhamahapatra, N. Sutradhar, M. Ghosh, H.C. Bajaj, A.B. Panda, Mesoporous sulfated zirconia mediated acetalization reactions, *Appl. Catal.A: Gen.* 402 (2011) 87–93.
24. X. Dou, D. Mohan, C.U. Pittman Jr., S. Yang, Remediating fluoride from water using hydrous zirconium oxide, *Chem. Eng. J.* 198-199 (2012) 236-245
25. D. Radwan, L. Saad, S. Mikhail, S.A. Selim, Catalytic Evaluation of Sulfated Zirconia Pillared Clays in *n*-Hexane Transformation, *J. Appl. Sci. Res.* 5 (12) (2009) 2332–2342.
26. V. Vishwanathan, G. Balakrishna, B. Rajesh, V. Jayasri, L.M. Sikhwivhilu, N.J. Coville, Alkylation of catechol with methanol to give guaiacol over sulphate-modified zirconia solid acid catalysts: The influence of structural modification of zirconia on catalytic performance, *Catal. Commun.* 9 (2008) 2422–2427.

27. M.T. Tran, N.S. Gnep, G. Szabo, M. Guisnet, Influence of the calcination temperature on the acidic and catalytic properties of sulphated zirconia, *Appl. Catal. A: Gen.* 171 (1998)207–217.
28. M.K. Mishra, B. Tyagi, R.V. Jasra, Synthesis and characterization of nano-crystalline sulfated zirconia by sol–gel method, *J. Mol. Catal. A: Chem.* 223 (2004) 61–65.
29. V.G. Deshmane, Y.G. Adewuyi, Mesoporous nanocrystalline sulfated zirconia synthesis and its application for FFA esterification in oils, *Appl. Catal. A: Gen.* 462 (2013) 196–206.
30. S.J. Gregg and K.S.W. Sing, Adsorption, Surface Area and Porosity *2nd ed. (Academia Press, London)* (1982) 195.
31. S. Wang, L. Zhao, W. Wang, Y. Zhao, G. Zhang, X. Ma and J. Gong,, Morphology control of ceria nanocrystals for catalytic conversion of CO<sub>2</sub> with methanol, *Nanoscale*, 5(2013) 5582-5588.
32. A. Kumar, S. Singhal, S. Agarwal, R.P.Badoni, K.M.Reddy, Synthesis and characterization of SiO<sub>2</sub>-Al<sub>2</sub>O<sub>3</sub> composite: Structural and surface properties, *J. of chem.phar. res.* 7(12) (2015) 328-335.
33. T. Sato, The thermal decomposition of zirconium oxyhydroxide *J. Therm. Anal. Calorim.* 69 (2002) 255–265.
34. R. Srinivasan, D. Taulbee, B. H. Davis, The effect of sulphate on the crystal structure of zirconia, *Catal. Lett.* 9 (1991) 1–7.
35. H. A. Khalaf, Textural properties of sulfated iron hydroxide promoted with aluminum, *Monatsh. Chem.* 140 (2009) 669–674.
36. B. M. Reddy, P. M. Sreekanth, P. Lakshmanan, A. Khan, Synthesis, characterization and activity study of SO<sub>4</sub><sup>2-</sup>/C<sub>x</sub>Zr<sub>1-x</sub>O<sub>2</sub> solid superacid catalyst, *J. Mol. Catal. A Chem.* 244 (2006) 1–7.

\*\*\*\*\*